A NEW HYPERSPECTRAL INDEX FOR CHLOROPHYLL ESTIMATION OF A FOREST CANOPY: AREA UNDER CURVE NORMALISED TO MAXIMAL BAND DEPTH BETWEEN 650-725 NM

Zbyněk Malenovský[1,2], Christian Ufer[1], Zuzana Lhotáková[3], Jan G.P.W. Clevers[1], Michael E. Schaepman[1], Jana Albrechtová[3] and Pavel Cudlín[2]

1. Wageningen University, Centre for Geo-Information, Wageningen, The Netherlands; {zbynek.malenovsky / christian.ufer / jan.clevers / michael.schaepman}(at)wur.nl
2. Academy of Sciences of the Czech Republic, Institute of Systems Biology and Ecology, Department of Forest Ecology, České Budějovice, Czech Republic; pavelcu(at)dale.uek.cas.cz
3. Charles University, Faculty of Science, Department of Plant Physiology, Prague, Czech Republic; zuza.lhotak(at)seznam.cz , albrecht(at)natur.cuni.cz

ABSTRACT

Total chlorophyll (C_{ab}) content of a forest canopy is used as indicator for the current state of a forest stand, and also as an input for various physiological vegetation models (i.e. models of photosynthesis, evapo-transpiration, etc.). Recent hyperspectral remote sensing allows retrieving the C_{ab} concentration of vegetation using the appropriate optical indices, and/or by means of biochemical information, scaled up from leaf to canopy level within radiative transfer (RT) models. Plenty of chlorophyll optical indices can be found in the literature for the leaf level, nevertheless, only some of them were proposed for a complex vegetation canopy like a forest stand. A robust chlorophyll optical index at the canopy level should be driven by the C_{ab} concentration without negative influence of other factors represented by soil background or understory, canopy closure, canopy structure (e.g. leaf area index (*LAI*), clumping of leaves), etc.

A new optical index named Area under curve Normalised to Maximal Band depth between 650-725 nm ($ANMB_{650\text{-}725}$) is proposed to estimate the chlorophyll content of a Norway spruce (*Picea abies*, /L./ Karst.) crown. This index was designed to exploit modifications of a vegetation reflectance signature invoked within the red-edge wavelengths mainly by the changes in leaf chlorophyll content. $ANMB_{650\text{-}725}$ is based on the reflectance continuum removal of the chlorophyll absorption feature between wavelengths of 650-725 nm. Suitability of the index and sensitivity on disturbing factors was tested using a 3D Discrete Anisotropic Radiative Transfer (DART) model coupled with a leaf radiative transfer model PROSPECT adjusted for spruce needles. The results of the $ANMB_{650\text{-}725}$ abilities within a coniferous forest canopy were compared with the performance of the chlorophyll indices ratio *TCARI*/*OSAVI*.

Test results, carried out with the DART model simulating hyperspectral data with 0.9 m pixel size, showed a strong linear regression of the $ANMB_{650\text{-}725}$ on spruce crown C_{ab} concentration (R^2=0.9798) and its quite strong resistance against varying canopy structural features such as *LAI* and canopy closure. The root mean square error (*RMSE*) between real and the $ANMB_{650\text{-}725}$ estimated C_{ab} concentrations was only 9.53 μg/cm^2 while the RMSE generated from prediction of the *TCARI*/*OSAVI* was two times higher (18.83 μg/cm^2). Chlorophyll retrieval using the $ANMB_{650\text{-}725}$ index remained stable also after introduction of two reflectance signal disturbing features: a) 20% of the spectral information of epiphytic lichen (*Pseudevernia* sp.) regularly distributed within the spruce canopy, and b) simulation of the sensor noise (computed for a signal to noise ratio equal to 5). *RMSE* of predicted C_{ab} concentration after the introduction of lichens appeared to be 10.51 μg/cm^2 and the combined influence of lichen presence and sensor noise in the image caused an increase of the *RMSE* to 12.13 μg/cm^2.

Keywords: hyperspectral quantitative remote sensing, chlorophyll optical index $ANMB_{650\text{-}725}$, DART, radiative transfer model.

INTRODUCTION

Current approaches of quantitative remote sensing allow to estimate the concentration of biochemical constituents spatially using fine spectral resolution (hyperspectral) image data in combination with radiative transfer models (1,2,3,4). One of the most important biochemical parameters of the vegetation canopy is the total concentration of the green foliar pigments, chlorophyll *a* and *b* (C_{ab}). Chlorophyll concentration of the forest canopy can be used as a biomarker for an acute environmental stress (5), as well as an input for physiological ecosystem models, for instance models estimating the photosynthetic efficiency (6).

A number of optical indices for estimating the leaf C_{ab} content was proposed (7), but not all of them are suitable to be used on the level of the complex forest canopy. A forest canopy is rather a spatially heterogeneous system, assembled from a certain amount of leaves and woody twigs (shoots in case of conifer species), branches of several orders, stems, and other components, arranged in the 3D space in a specific way. Therefore, any optical index, designed for estimation of the biochemical parameter, should be preferably driven only by the concentration of this biochemical constituent, and be independent of other structural and biochemical characteristics of the canopy (e.g. density and distribution of leaves, canopy closure, etc.) including surrounding environment (e.g. influence of understory and soil on background).

Radiative transfer (RT) models represent an ideal tool to design and test such biochemical optical indices. Haboudane et al. (8) gave a typical example of how the RT models can be used for development of an optical index performing optimally on the canopy scale. They employed the leaf RT model PROSPECT coupled with the SAILH canopy RT model to establish and test the ratio of two optical indices *TCARI* (9) and *OSAVI* (10) as an appropriate vegetation index for estimation of agriculture canopy C_{ab} content from hyperspectral imagery. The *TCARI*/*OSAVI* ratio, simulated for a corn field, was shown to be a robust chlorophyll biomarker, minimally influenced by the reflectance of the underlying soil and the variation in the canopy *LAI* (11).

A similar technique, employing the RT models PROSPECT and DART (Discrete Anisotropic Radiative Transfer), was applied in our study to develop and test the sensitivity of a robust chlorophyll estimating optical index for a heterogeneous coniferous forest canopy. A newly proposed index named Area under curve Normalised to Maximal Band depth between 650-725nm ($ANMB_{650\text{-}725}$) is based on the method called continuum removal of reflectance spectra (4), using advantages of fine spectral resolution and sampling band interval of the hyperspectral images acquired with a very small pixel-size. The continuum removal technique was lately used over aerial hyperspectral data by Underwood et al. (12) for mapping specific invasive plants, and by Kokaly et al. (13) for discriminating different vegetation cover types in the Yellowstone National Park, as well as by Schmidt and Skidmore (14) to differentiate saltmarsh vegetation types of the Dutch Waddenzee wetland. Already in 1999, Kokaly and Clark used normalised band depths calculated from specific continuum-removed absorption features of reflectance, measured over dried and ground leaves, to estimate the concentrations of nitrogen, lignin, and cellulose. Curran et al. (15) refined the Kokaly and Clark methodologies combining band depths normalised to the wavelength at the centre of the absorption feature (*BNC*) or the area of the absorption feature (*BNA*) with stepwise multiple linear regression. They used these spectral parameters to assess concentrations of C_{ab} within two absorption features: 408-518nm, and 588-750nm.

METHODS

Design of the $ANMB_{650\text{-}725}$ index

The new chlorophyll estimating optical index $ANMB_{650\text{-}725}$ is based on the continuum removal of the chlorophyll absorption feature at the red-edge part of the spectrum, i.e. between the wavelengths of 650-725 nm. The logic behind this spectral index is exploiting well known changes of a vegetation reflectance signature shape invoked within these wavelengths mainly by the changes in leaf chlorophyll content (Figure 1). An increase in the chlorophyll concentration causes the chlorophyll absorption feature to deepen at the red-edge of reflectance with the absorption maximum at approximately 675-680 nm (Figure 1a). The reflectance at maximum chlorophyll absorption becomes

saturated with increasing C_{ab} concentration (9), but the adjacent wavebands (especially of longer wavelengths) remain very sensitive to these changes. Therefore, the area under a continuum-removed reflectance curve from 650 to 725 nm is getting significantly smaller with a declining chlorophyll content, and the maximal band depth of this area is systematically changing, too (Figure 1b).

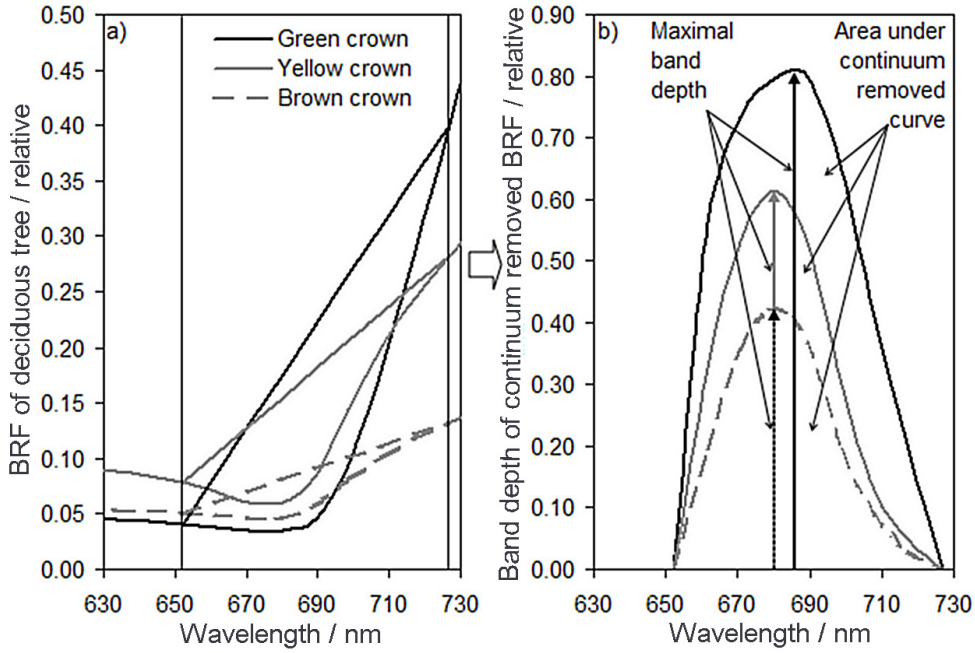

Figure 1: Description of continuum removal and band depth calculation to generate the $ANMB_{650\text{-}725}$ *index from sunlit vegetation spectral signatures of a "green" (high* C_{ab}*), "yellow" (very low* C_{ab}*), and "brown" (dead tree without* C_{ab}*) coloured crown of a deciduous tree extracted from an AISA Eagle atmospherically corrected hyperspectral image; a) delineation of the reflectance feature at the chlorophyll absorption between 650 and 725 nm; b) maximal band depth (*$MBD_{650\text{-}725}$*) and area under reflectance continuum-removed curve (*$AUC_{650\text{-}725}$*).*

Based on this observation, the continuum removal procedure (16) is applied on the canopy bidirectional reflectance factor (*BRF*) of wavelengths between 650 and 725 nm as first step of the $ANMB_{650\text{-}725}$ computation. Secondly, the area under the continuum-removed reflectance curve between 650 and 725 nm ($AUC_{650\text{-}725}$) is integrated according to the equation:

$$AUC_{650-725} = \frac{1}{2}\sum_{j=1}^{n-1}(\lambda_{j+1} - \lambda_j)(\rho_{j+1} + \rho_j) \ , \qquad (1)$$

where ρ_j and ρ_{j+1} are values of the continuum-removed reflectance at the *j* and *j*+1 bands, λ_j and λ_{j+1} are wavelengths of the *j* and *j*+1 bands, and *n* is the number of the used spectral bands. Finally, the $ANMB_{650\text{-}725}$ index is computed as:

$$ANMB_{650\text{-}725} = \frac{AUC_{650\text{-}725}}{MBD_{650\text{-}725}}, \qquad (2)$$

where $MBD_{650\text{-}725}$ is a maximal band depth of the continuum-removed reflectance, placed at one of the spectrally stable wavelengths of strongest chlorophyll absorption around 675-680 nm. Normalisation of $AUC_{650\text{-}725}$ by $MBD_{650\text{-}725}$ is a crucial step ensuring a strong relationship between $ANMB_{650\text{-}725}$ and the chlorophyll content at higher concentrations. The dependence relation of $AUC_{650\text{-}725}$ on the C_{ab} concentration saturates for C_{ab} > 60 μg/cm^2, while values of the $MBD_{650\text{-}725}$ above this C_{ab} concentration start to systematically decrease. This disproportional non-linear relationship between

the $AUC_{650\text{-}725}$ and the $MBD_{650\text{-}725}$ makes their ratio, i.e. the $ANMB_{650\text{-}725}$ index, sensitive to not only low and average, but also to high concentrations of C_{ab}.

Radiative transfer models

The PROSPECT model, adopted for Norway spruce (*Picea Abies* (L.) Karst.) needles, and the canopy radiative transfer model DART were combined to simulate airborne very high spatial resolution hyperspectral images of a mature spruce forest stand, and subsequently to generate the BRF database of sunlit crown spectral signatures (see flowchart in Figure 2).

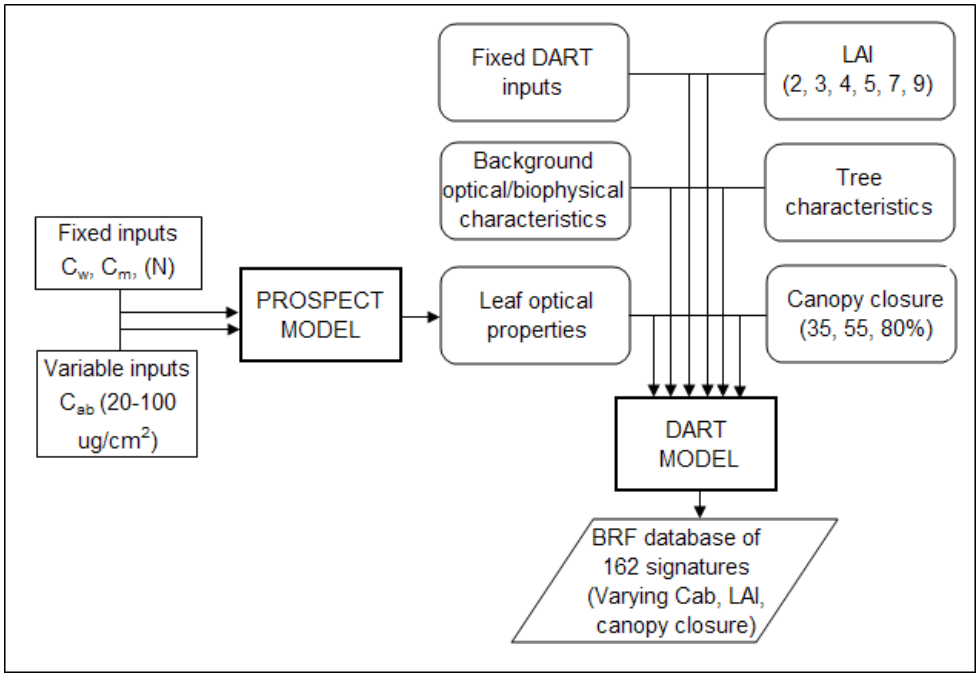

Figure 2: Flowchart illustrating the creation of the BRF database used to develop the $ANMB_{650\text{-}725}$ index, and to establish its statistical relationship with chlorophyll content.

The PROSPECT model (17) simulates leaf hemispherical reflectance and transmittance signatures from 400 to 2500 nm as a function of leaf structural parameters and leaf biochemical components. Scattering is described by a specific refractive index (n) and a parameter characterising the leaf mesophyll structure (N). Absorption is modelled using pigment concentration (C_{ab}), water content (C_w), dry matter content (C_m) and the corresponding specific spectral absorption coefficients (k_{ab}, k_w, and k_m). PROSPECT was adjusted to simulate properly spectral properties of the Norway spruce needles by means of the measured leaf hemispherical directional optical, biochemical and structural characteristics (18). PROSPECT outputs were directly used in the DART model to simulate the bidirectional reflectance factor (*BRF*) (19) at the top of the canopy (*TOC*).

DART is a 3D radiative transfer model, based on the discrete ordinance method and an iterative approach. A simulated landscape scene is represented as a rectangular solid medium of adjacent cells forming a 3D matrix. Each cell of the matrix is identified with the x, y and z coordinates at the centre point. Cells can create different types of scene elements, classified as opaque or solid cells (e.g. soil or water) and semi-opaque or turbid cells (e.g. leaves of vegetation), which can vary in spatial dimensions. Each of them requires specific optical and structural characteristics, for instance leaf area index, leaf angle distribution, and optical reflectance/transmittance functions in case of vegetation foliage. The 3D radiation regime and the canopy BRF are realistically generated by considering topography, major physical mechanisms (e.g. hotspot effect), surface optical properties and four types of scattering. A detailed description of the DART algorithm and functions is available in Gascon et al. (20), Gastellu-Etchegorry et al. (21), and Gastellu-Etchegorry et al. (22).

Parameterisation of the RT models and generation of the BRF database

The RT models were parameterised using the data acquired during September 2003 within the field survey of the Norway spruce forest stands situated near the village Modrava (48°59'N, 13°28'E), at the Sumava Mts. National Park (Czech Republic). The main information collected in the frame of this field campaign is shown in Table 1. Heterogeneous representative 3D scenes of three canopy closures were generated out of averages and standard deviations of the tree field measurements. Clumping of the foliage within the branches was simulated as a combination of systematic and random propagation of the "gaps" (empty "air" cells) within the tree canopy. This calibration was based on the visual observation of the crown defoliation and laboratory destruction of 16 representative branches. Ground surface was represented by a flat surface (digital elevation model was not included) covered by the most frequent mountain grass *Calamagrostis villosa*. Mean allometric characteristics of the examined representative trees used for the BRF database simulation are described in Table 2. Leaf optical properties were generated in the adjusted PROSPECT model as weighted averages of spectral properties of the last three needle generations (age weights were calculated from the branch destruction). 78 needle samples from 13 selected trees were analysed in this respect to obtain the following average input values: C_w = 0.06 cm, C_m = 0.026 g/cm^2, N = 2.15.

Table 1: Basic inputs acquired for the radiative transfer simulations of the Norway spruce stands of Sumava Mts. in Czech Republic.

Thematic class	Measured variables	Measuring methods and devices
Bio-metric parameters of sampled trees	Tree positions, total trunk height, height of crown, horizontal crown projection, vertical crown profile, trunk diameters, length of live and dead crown, etc.	Digital forest mapping system FieldMap connected to the Impulse 200 Laser Rangefinder and the MapStar electronic compass.
Bio-physical parameters of crown	Leaf area index (*LAI*) per crown. Foliage density distribution – clumping of the leaves within crown.	Li-Cor plant canopy analyser (PCA) LAI-2000. Laboratory destruction of 16 sample branches.
Spectral properties	Hemispherical-directional optical properties of major forest stand surfaces (trunk bark, branch bark, understory, bare soil, rock, etc.)	Li-Cor spectroradiometer LI-1800-22 coupled with an integrating sphere LI-1800-12.

Table 2: Universal tree characteristics used for building the BRF database.

Length of trunk / m		Trunk diameter / m		Length of crown / m	Crown radius /m	
Outside of crown	Inside of crown	Outside of crown	Inside of crown		Lower part	Upper part
7.75	9.20	0.36	0.19	13.50	2.70	0.00

Finally, 162 DART simulations were performed to obtain the top of the canopy *BRF* database of the virtual Norway spruce stands through all possible combinations of the following varying inputs: *LAI* (2, 3, 4, 5, 7, and 9), C_{ab} content (20, 30, 40, 50, 60, 70, 80, 90, 100 µg/cm^2), and % of canopy closure (*CC*) (35, 55, and 80%). The solar illumination direction was defined by the azimuth angle of 181.2°and zenith angle of 42.2° (real solar noon on September 15th). Outputs were reproducing the hyperspectral images as potentially captured by the AISA airborne sensor (Specim Ltd., Finland) in the 'spatial' acquisition mode. This mode of the first AISA generation allowed very high spatial resolution of 0.9 m, compulsory for separation of the individual tree crowns, but only for a limited number of the equally spaced spectral bands. Thus, 18 spectral bands meeting the AISA standards in full-width-half-maximum (*FWHM*) and spectral sampling interval were simulated (Table 3). In the final step only spectral signatures of sunlit crown pixels of spectral bands from 648 to 726 nm were extracted to build the *BRF* database necessary for the chlorophyll $ANMB_{650\text{-}725}$ establishment. The *BRF* of sunlit crowns at 552 and 800 nm was additionally stored in the database for

computing the chlorophyll predicting index *TCARI/OSAVI* (8), used in performance validation. The sunlit crown pixels were selected based on the reflectance thresholds of three channels (552, 671, and 800 nm). These thresholds were determined visually on a limited number of crowns and then applied automatically within the remaining crowns. Unfortunately, this approach caused a slight misclassification at the border of both classes, resulting in inclusion of a few shaded pixels into the class of sunlit. Hence, this approach should be in future exchanged for an automatic segmentation algorithm with higher accuracy.

Table 3: Spectral description of simulated AISA bands.

Band No.	Central λ /nm	FWHM /nm	Band No.	Central λ /m	FWHM /nm
1	452.6	7.3	10	671.3	7.6
2	474.5	7.3	11	700.2	7.6
3	496.4	7.3	12	726.0	7.6
4	524.0	7.3	13	748.8	7.6
5	551.7	7.3	14	780.7	7.6
6	576.5	7.3	15	800.4	7.6
7	601.2	7.3	16	844.5	7.6
8	624.6	7.3	17	861.2	7.6
9	648.5	7.6	18	870.3	7.6

$ANMB_{650\text{-}725}$ validation and sensitivity analysis

Three real forest research plots, selected within the mature Norway spruce stands at the Sumava Mts. National Park, were modelled in the DART model for validation of the $ANMB_{650\text{-}725}$. DART landscape representatives were prepared using a FieldMap digital forest mapping system (IFER Ltd., Czech Republic) coupled with the Laser Rangefinder Impulse 200 and the MapStar electronic compass (Laser Technology Inc., USA) (for example of a forest input map, see Figure 3). Realistic scenes contained 13 sample trees, several neighbourhood adult and young trees, lying dead wood, and vegetation understory combined with litter of senescent spruce needles and bare soil. Hemispherical directional optical properties of needles and major scene surfaces were measured with the Li-Cor spectroradiometer LI-1800-22 connected to an integrating sphere LI-1800-12 (Li-Cor Inc., USA) (23). Structural parameters of the forest stands were set in a similar way as for the BRF database scenes.

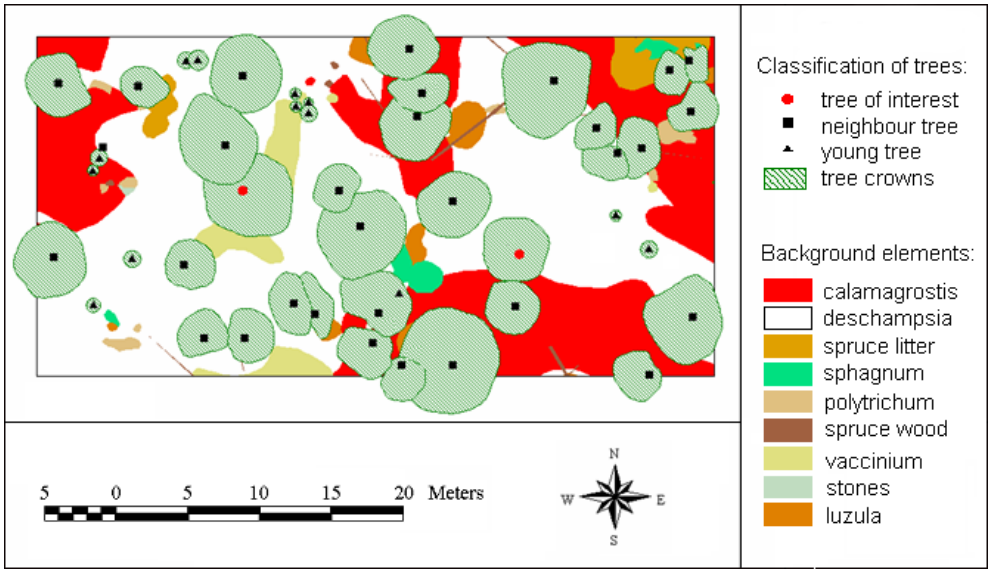

Figure 3: Map of one research plot at the Sumava Mts. National Park (Czech Republic) used in DART to generate hyperspectral images for accuracy assessment of the $ANMB_{650\text{-}725}$ index.

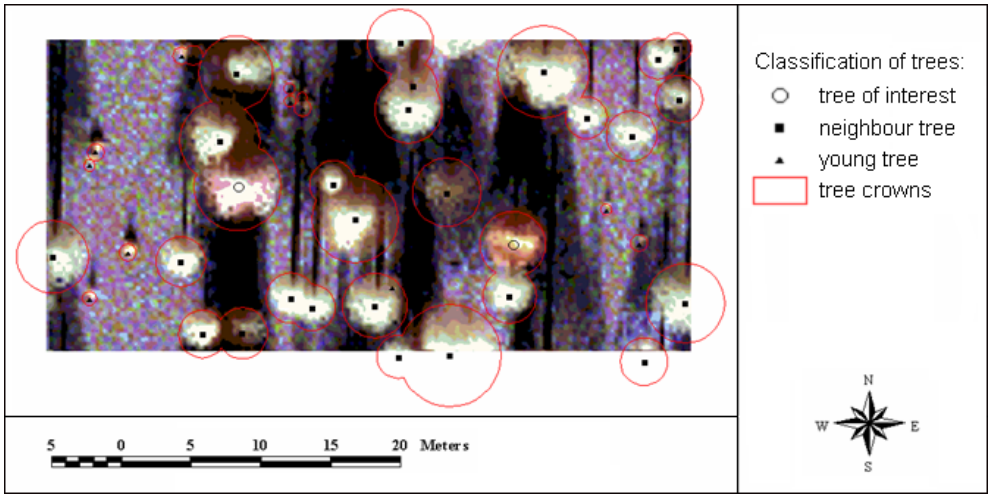

Figure 4: A false colour RGB composition of DART simulated nadir AISA bands (R=800 nm, G=552 nm and B=681 nm) for the research plot depicted in Figure 3.

The total concentrations of the chlorophyll *a* and *b* (C_{ab}) for 99 collected samples of current, two and three year old needles were determined spectrophotometrically in the laboratory. A Unicam Helios α spectrophotometer (Unicam Ltd., UK) was used according to the methodology of Porra et al. (24) and Wellburn (25) for this purpose. The proper needle age-class ratio of chlorophyll concentrations was up-scaled by the adjusted PROSPECT-DART model into the TOC BRF AISA hyperspectral images of observed spruce stands (Figure 4). $ANMB_{650\text{-}725}$ was derived from spectral signatures of sunlit crown pixels of 13 sample trees (see Table 4). The equation of linear regression, established between $ANMB_{650\text{-}725}$ and C_{ab} concentration from the *BRF* database, was applied to estimate their C_{ab} values. Finally, the root mean square error (*RMSE*) was computed between retrieved and true C_{ab} concentrations to assess the accuracy of the $ANMB_{650\text{-}725}$ estimation.

Table 4: Biophysical and biochemical properties of 13 sample spruce crowns simulated in DART for the sensitivity analyses of $ANMB_{650\text{-}725}$.

ID of sample tree	% of crown defoliation	Leaf area index (*LAI*)	Chlorophyll content / µg/cm^2
24	35	9.18	81.79
25	45	8.87	68.99
11	45	7.24	43.41
21	45	6.59	93.55
16	45	6.32	74.15
29	50	7.26	55.13
22	50	4.85	81.74
10	55	5.82	63.16
5	60	4.37	60.40
15	60	3.94	47.96
8	60	3.73	27.56
6	60	1.16	58.94
17	65	3.43	77.90

The performance of the $ANMB_{650\text{-}725}$ optical index was also compared with C_{ab} prediction abilities of the optical ratio TCARI/OSAVI. Haboudane et al. (8) proposed the ratio of the Transformed Chlorophyll Absorption in Reflectance Index (*TCARI*) and the Optimised Soil-Adjusted Vegetation Index (*OSAVI*) (26) as strongly sensitive to chlorophyll concentration and highly resistant to the variations of *LAI* (Leaf Area Index) and solar zenith angle at the canopy level. The TCARI is a transformed

variant of the chlorophyll index MCARI (Modified Chlorophyll Absorption in Reflectance Index) (9), defined as follows:

$$TCARI = 3\left[\left(\rho_{700} - \rho_{670}\right) - 0.2\left(\rho_{700} - \rho_{550}\right)\left(\frac{\rho_{700}}{\rho_{670}}\right)\right]. \quad (3)$$

The *OSAVI* index, belonging to the family of soil line vegetation indices (10), can be computed by the equation:

$$OSAVI = \frac{(1+0.16)(\rho_{800} - \rho_{670})}{(\rho_{800} + \rho_{670} + 0.16)}, \quad (4)$$

where ρ_j is the reflectance value at the *j*-th wavelength in nanometres; $j \in$(550, 670, 700, 800).

Finally, a sensitivity analysis of the $ANMB_{650\text{-}725}$ C_{ab} predictability on the presence of epiphytic lichens within the canopy (scenario #1) and added sensor noise (scenario #2) was performed. Scenario #1 was realised by changing the optical properties of the trees of interest in the DART model. Based on visual observation, 20% of the measured hemispherical optical properties of most common lichen at the Sumava spruce forests, *Pseudevernia* sp., were spectrally mixed with 80% of the original needle optical properties. Scenario #2 was simulated by adding a certain level of noise to the simulated image of scenario #1. The noise simulated in this work tries to resemble only the noise caused by a detector. The fact that each hyperspectral system is recording an image by counting photons allows the assumption that this noise can be modelled with an independent, additive model: the noise *n(i,j)* has a zero-mean Gaussian distribution described by its standard deviation and/or variance. This means that each pixel in the noisy image is the sum of the true pixel value and the random Gaussian distributed noise value (σ_n^2). The intensity of sensor noise in an image is described by the signal to noise ratio (*SNR*), which is given by:

$$SNR = \sqrt{\frac{\sigma_f^2}{\sigma_n^2} - 1} \quad (5)$$

where, σ_f^2 is the variance of the real recorded image (in our case the image of scenario #1 plus noise) and σ_n^2 is the variance of the zero-mean noise image (27). The SNR value was set to five to simulate noise with a standard deviation σ_n ~ 20% of the true image standard deviation σ_s. Then the σ_n was computed from:

$$\sigma_n = \frac{\sigma_s}{SNR} \quad (6)$$

The IDL function 'gen_image_doit' was used to generate an image with zero-mean noise of σ_n distributed by the Gaussian function per each spectral band. Then the appropriate noisy images were summed up with the image spectral bands of scenario #1.

RESULTS

Figure 5a shows the exponential regression of the integrated area under continuum-removed reflectance curve between 650 and 725 nm ($AUC_{650\text{-}725}$) on the canopy chlorophyll concentration computed out of the *BRF* database. The $AUC_{650\text{-}725}$ values saturate for a C_{ab} concentration above 60 μg/cm^2 which means $AUC_{650\text{-}725}$ is not able to resolve a C_{ab} content higher than 60 μg/cm^2. On the other hand, the maximal band depth of continuum-removed canopy reflectance between 650-725 nm ($MBD_{650\text{-}725}$) is steeply growing with an increase of the C_{ab} concentration up to 60 μg/cm^2, gains the maximal values at this C_{ab} concentration, and decreases for a C_{ab} content above 60 μg/cm^2 (Figure 5b). Consequently, the proposed reciprocal ratio of these two optical parameters ($ANMB_{650\text{-}725}$) exhibits a strong linear relationship with the total canopy chlorophyll concentration. The variability in $ANMB_{650\text{-}725}$ due to varying LAI and canopy closure is rather low. One can see in

Figure 6a that the $ANMB_{650\text{-}725}$ values for the specified C_{ab} concentration levels with a basic step of 10 μg/cm^2 did not overlap, except for three outliers. This suggests a low sensitivity of the $ANMB_{650\text{-}725}$ index on the structural parameters of the simulated spruce canopy. The three outliers result from misclassification of the sunlit crown pixels. Some of the crown shaded pixels with higher portion of noise were included into the sunlit crown signature causing a non-systematic shift of the $ANMB_{650\text{-}725}$ values.

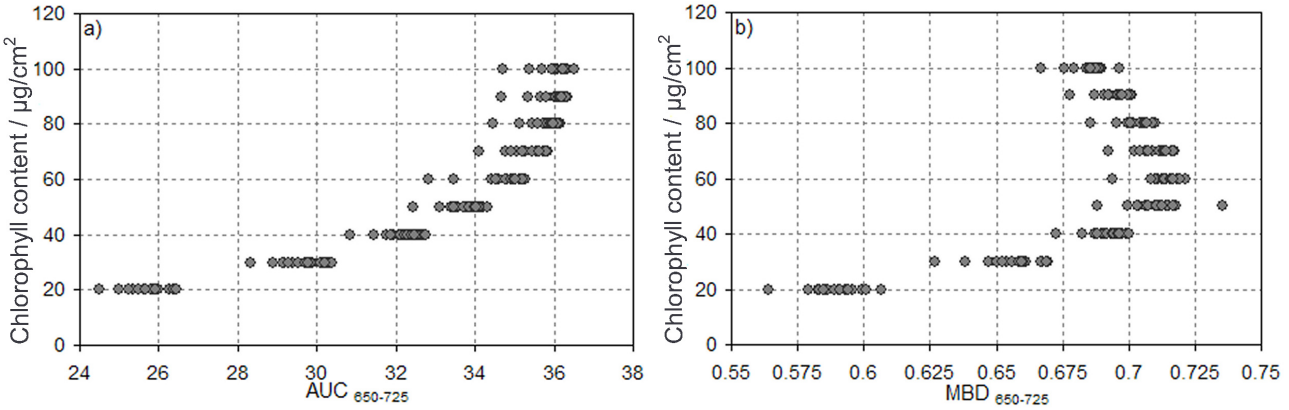

Figure 5. Relationship of the optical parameters and canopy chlorophyll concentration computed from the BRF *database; a) Integrated area under continuum-removed reflectance between 650 and 725 nm (*$AUC_{650\text{-}725}$*); b) Maximal band depth of continuum-removed reflectance between 650 and 725 nm (*$MBD_{650\text{-}725}$*).*

The statistical relation of the C_{ab} content and $ANMB_{650\text{-}725}$ obtained from the *BRF* database is highly significant (r^2=0.9798) and comparable with the relationship between C_{ab} concentration and the ratio *TCARI*/*OSAVI* (r^2=0.9731) (c.f. Figure 6ab). However, the final C_{ab} concentration for 13 sample trees estimated by means of both optical indices differs in accuracy. Plots of Figure 7 and RMSE values computed between assessed and measured C_{ab} concentrations show considerably higher prediction accuracy for the $ANMB_{650\text{-}725}$ (*RMSE*=9.53 μg/cm^2) than for the *TCARI*/*OSAVI* index (*RMSE*=18.83 μg/cm^2). Subsequently, the coefficient of determination for a linear regression, established between measured and estimated C_{ab}, is high for $ANMB_{650\text{-}725}$ (r^2=0.7178) and quite low for *TCARI*/*OSAVI* (r^2=0.1695). These results suggest an appropriate and generally acceptable accuracy of the $ANMB_{650\text{-}725}$ chlorophyll content prediction from sunlit forest canopy pixels of very high spatial resolution.

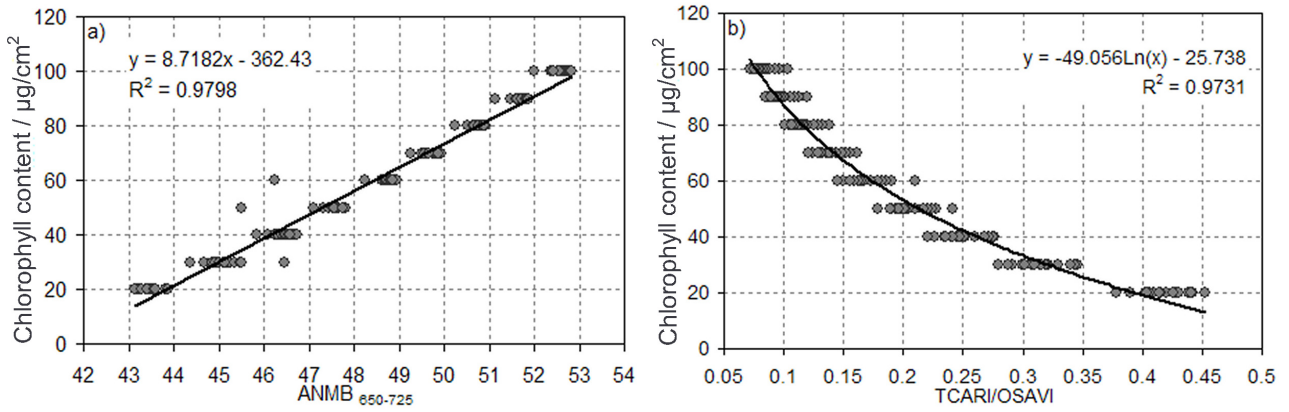

Figure 6: Statistical relationships between chlorophyll concentration and chlorophyll optical indices generated from the BRF database; a) Linear regression of canopy C_{ab} *concentration on the area under curve normalised to maximal band depth between 650 and 725 nm (*$ANMB_{650\text{-}725}$*); b) Logarithmic statistical relationship of* C_{ab} *concentration and the optical indices ratio* TCARI/OSAVI*.*

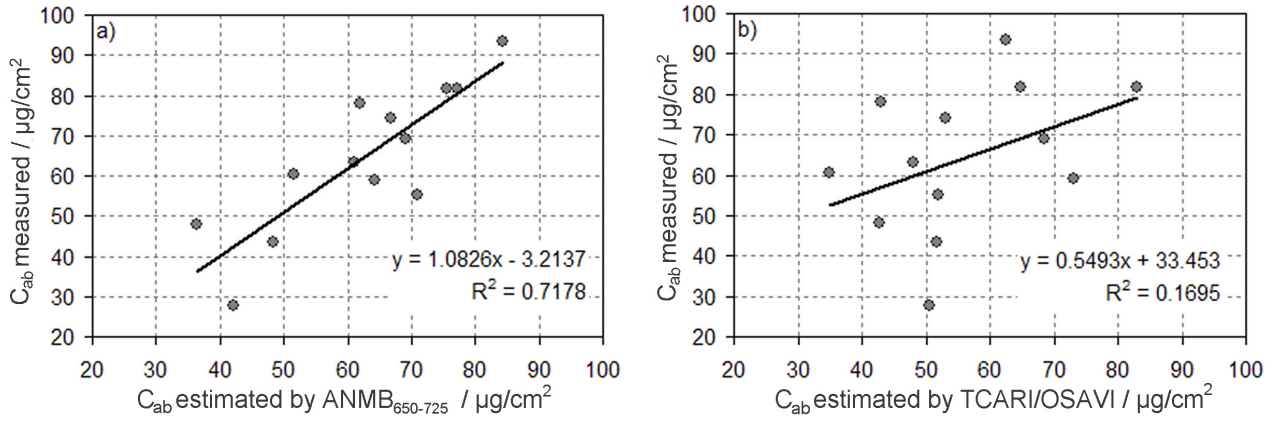

Figure 7: One-to-one relationship and linear regression of chlorophyll concentration measured for 13 sample spruce crowns and estimated by the optical index; a) $ANMB_{650\text{-}725}$*; b)* TCARI/OSAVI*.*

The introduction of 20% of an epiphytic lichen spectral signature into the canopy optical properties of the sample spruce trees did not result in a significant decrease of the $ANMB_{650\text{-}725}$ estimation accuracy (*RMSE*=10.51 µg/cm²; r^2=0.6689). As expected, simulated combined influence of the lichen occurrence within the crowns with the computer-generated sensor noise (*SNR*=5) caused a decline in the $ANMB_{650\text{-}725}$ prediction accuracy (*RMSE*=12.13 µg/cm²; r^2=0.5325), but the accuracy was still higher than for the *TCARI*/*OSAVI* estimation without any disturbing effects. However, it has to be stressed that the $ANMB_{650\text{-}725}$ index is computed as a *BRF* shape parameter through the wavelengths of the high C_{ab} absorption feature, which means within a quite low reflectance signal. Any noise significantly weakening the signal and disturbing the shape of the reflectance curve will cause a decrease of the chlorophyll prediction ability. Hence, sunlit crown pixels with a strong reflectance signal must be separated from noisy shadowed pixels and only these can be used for $ANMB_{650\text{-}725}$ computation, otherwise index predictability is reduced (see outliers in Figure 6a). Therefore, further testing and more sensitivity analyses, including other kinds of noise, more variations of spectral resolution and band sampling interval, and also lower spatial resolution, are required in order to show stability and full reliability of the $ANMB_{650\text{-}725}$ hyperspectral index for C_{ab} concentration estimation.

CONCLUSIONS

A new optical index $ANMB_{650\text{-}725}$ for estimating the canopy chlorophyll concentration from hyperspectral remote sensing data of a very high spatial resolution was proposed and causally explained. The $ANMB_{650\text{-}725}$ is based on qualitative (shape) information of the vegetation reflectance curve rather than on the quantitative changes of reflectance intensity driven by the total chlorophyll content. First tests and a sensitivity analysis of the $ANMB_{650\text{-}725}$ proved its robustness and acceptable prediction accuracy for heterogeneous spruce crowns contrary to the *TCARI*/*OSAVI* index, which was originally designed for agricultural crops. Computation of the index, using only four wavebands with the $MBD_{650\text{-}725}$ always at channel 671.3 nm due to the low spectral sampling interval, did not reduce the $ANMB_{650\text{-}725}$ estimation capability. Even the introduction of two disturbing effects, occurrence of spruce epiphytic lichen *Pseudevernia* sp., and simulation of a low signal-to-noise ratio of 5:1 within the hyperspectral image data did not change radically the index performance.

Nevertheless, further sensitivity analyses of this new chlorophyll optical index are recommended to be carried out on real hyperspectral imagery of higher spectral sampling interval. The results of estimation should be verified against real ground truth measurements of canopy chlorophyll concentrations.

Finally, the $ANMB_{650\text{-}725}$ index was developed and so far applied only on the Norway spruce stands. Therefore, it must also be tested and validated for the other plant species and functional plant types, especially broad-leaved species with different leaf interior and architecture of the canopy.

ACKNOWLEDGEMENTS

The authors are grateful to Jean-Philippe Gastellu-Etchegorry and Emmanuel Martin from the CESBIO Laboratory (France) for the opportunity to use the DART model for this study. They are also thankful for the PROSPECT model source code provided by Stephane Jacquemoud (Universite Paris 7, France). Zbyněk Malenovský acknowledges financial support provided by the Czech Ministry of Education, Youth and Sports in the frame of the Sabbatical fellowship 1K04. The study was carried out within the Research Plan of the Institute of Systems Biology and Ecology: AVOZ60870520.

REFERENCES

1 Gamon J A, K F Huemmrich, D R Peddle, J Chen, D Fuentes, F G Hall, J S Kimball, S Goetz, J Gu & K C McDonald, 2004. Remote sensing in BOREAS: Lessons learned. Remote Sensing of Environment, 89(2): 139-162

2 Johnson L F, C A Hlavka & D L Peterson, 1994. Multivariate analysis of AVIRIS data for canopy biochemical estimation along the oregon transect. Remote Sensing of Environment, 47(2): 216-230

3 Peddle D R, R L Johnson, J Cihlar & R Latifovic, 2004. Large area forest classification and biophysical parameter estimation using the 5-Scale canopy reflectance model in Multiple-Forward-Mode. Remote Sensing of Environment, 89(2): 252-263

4 Broge N H & E Leblanc, 2001. Comparing prediction power and stability of broadband and hyperspectral vegetation indices for estimation of green leaf area index and canopy chlorophyll density. Remote Sensing of Environment, 76(2): 156-172

5 Malenovský Z, J G P W Clevers, H Arkimaa, V Kuosmanen, P Cudlín & T Polák, 2003. Spectral differences of the functional crown parts and status of Norway spruce trees studied using remote sensing. Ekologia (Bratislava), 22Supplement 1: 207-210

6 Curran P J, 1994. Attempts to drive ecosystem simulation models at local to regional scales. In: Environmental remote sensing from regional to globel scales, edited by G M Foody and P J Curran (Wiley & Sons) 149-166

7 Le Maire G, C Francois & E Dufrene, 2004. Towards universal broad leaf chlorophyll indices using PROSPECT simulated database and hyperspectral reflectance measurements. Remote Sensing of Environment, 89(1): 1-28

8 Haboudane D, J R Miller, N Tremblay, P J Zarco-Tejada & L Dextraze, 2002. Integrated narrow-band vegetation indices for prediction of crop chlorophyll content for application to precision agriculture. Remote Sensing of Environment, 81(2-3): 416-426

9 Daughtry C S T, C L Walthall, M S Kim, E de Colstoun & J E Brown McMurtreyIII, 2000. Estimating corn leaf chlorophyll concentration from leaf and canopy reflectance. Remote Sensing of Environment, 74(2): 229-239

10 Steven M D, 1998. The sensitivity of the OSAVI vegetation index to observational parameters. Remote Sensing of Environment, 63(1): 49-60

11 Zarco-Tejada P J, J R Miller, A Morales, A Berjon & J Aguera, 2004. Hyperspectral indices and model simulation for chlorophyll estimation in open-canopy tree crops. Remote Sensing of Environment, 90(4): 463-476

12 Underwood E, S Ustin & D DiPietro, 2003. Mapping nonnative plants using hyperspectral imagery. Remote Sensing of Environment, 86(2): 150-161

13 Kokaly R F, D G Despain, R N Clark & K E Livo, 2003. Mapping vegetation in Yellowstone National Park using spectral feature analysis of AVIRIS data. Remote Sensing of Environment, 84(3): 437-456

14 Schmidt K S & A K Skidmore, 2003. Spectral discrimination of vegetation types in a coastal wetland. Remote Sensing of Environment, 85(1): 92-108

15 Curran P J, J L Dungan & D L Peterson, 2001. Estimating the foliar biochemical concentration of leaves with reflectance spectrometry: Testing the Kokaly and Clark methodologies. Remote Sensing of Environment, 76(3): 349-359

16 Kokaly R F & R N Clark, 1999. Spectroscopic determination of leaf biochemistry using band-depth analysis of absorption features and stepwise multiple linear regression. Remote Sensing of Environment, 673: 267-287

17 Jacquemoud S & F Baret, 1990. Prospect - a model of leaf optical properties spectra. Remote Sensing of Environment, 34(2): 75-91

18 Malenovský Z, J Albrechtová, Z Lhotáková, R Zurita-Milla, J G P W Clevers, M E Schaepman & P Cudlín, 2006. Applicability of the PROSPECT model for Norway spruce needles. International Journal of Remote Sensing (in press)

19 Schaepman-Strub G, M Schaepman, S Dangel, T Painter & J Martonchik, 2005. About the use of reflectance terminology in imaging spectroscopy. EARSeL eProceedings, 4(2): 191-202

20 Gascon F, J P Gastellu-Etchegorry, M J Lefevre-Fonollosa & E Dufrene, 2004. Retrieval of forest biophysical variables by inverting a 3-D radiative transfer model and using high and very high resolution imagery. International Journal of Remote Sensing, 25(24): 5601-5616

21 Gastellu-Etchegorry J P, V Demarez, V Pinel & F Zagolski, 1996. Modeling radiative transfer in heterogeneous 3-D vegetation canopies. Remote Sensing of Environment, 58(2): 131-156

22 Gastellu-Etchegorry J P, E Martin & F Gascon, 2004. DART: a 3D model for simulating satellite images and studying surface radiation budget. International Journal of Remote Sensing, 25(1): 73-96

23 Li-Cor, 1983. 1800-12 Integrating sphere instruction manual. Publication number 8305-0034

24 Porra R J, W A Thompson & P E Kriedemann, 1989. Determination of accurate extinction coefficients and simultaneous equations for assaying chlorophylls a and b extracted with four different solvents: verification of the concentration of chlorophyll standards by atomic absorption spectroscopy. Biochimica and Biophysica Acta, 975(3): 384-394

25 Wellburn A R, 1994. The spectral determination of chlorophyll a and chlorophhyll b, as well as total carotenoids, using various solvents with spectrophotometers of different resolution. Journal of Plant Physiology, 144(3): 307-313

26 Rondeaux G, M Steven & F Baret, 1996. Optimization of soil-adjusted vegetation indices. Remote Sensing of Environment, 55(2): 95-107

27 Fisher B, S Perkins, A Walker & E Erik Wolfart, 1994. Hypermedia Image Processing Reference (Department of Artificial Intelligence, University of Edinburgh, UK)